Supplemental Information

Table S1. Relative sensitivity of lymphoblastoid cell lines to alkylating agents; **Table S2.** DNA repair capacity data for 24 cell lines. **Table S3.** Correlation coefficients for pairwise linear relationships between DNA repair capacity in multiple pathways in 24 lymphoblastoid cell lines. **Table S4.** Statistical significance of linear relationships between DNA repair capacity in multiple pathways in 24 lymphoblastoid cell lines. **Table S5.** Correlation coefficients for pairwise linear relationships between DNA repair capacity and sensitivity to killing with DNA damaging agents in 24 lymphoblastoid cell lines. **Table S6.** Statistical significance of linear relationships between DNA repair capacity and sensitivity to killing with DNA damaging agents in 24 lymphoblastoid cell lines. **Table S7**. DNA Repair capacity for indicated repair pathways in PDX models of GBM. **Figure S1.** Computational Workflow. **Figure S2.** Diagram of a linear model relating MGMT activity to sensitivity to MNNG. **Figure S3.** Correlation between MGMT activity (as measured by FM-HCR) and sensitivity to a DNA damaging agent. **Figure S4.** Scatter plots of observed sensitivity (% Control Growth) versus predicted sensitivity calculated from leave-one-out analysis of the models listed in **Table 1**. **Figure S5.** Predicted and observed sensitivity of paired GBM xenograft lines with differential TMZ sensitivities. **Figure S6.** Correlation between MGMT activity and promoter methylation status.

Repair pathways that contribute to S_N1 alkylating agent sensitivity

The quantitative models (#1-6) relating MGMT, MMR, HR and NER capacity to TMZ and MNNG sensitivity are consistent with previously established roles for DNA repair pathways affecting the sensitivity of cells to killing with S_N1-type alkylating agents (**Fig. 2**). MGMT directly reverses O^6-MeG to restore the native guanine base (1). Cancer cells expressing high levels of MGMT are resistant to TMZ, and conversely, MGMT promoter hypermethylation can silence MGMT expression in cancer cells (2), leading to hypersensitivity to TMZ and increased benefit from therapy (3,4). Thus, the models confirm the expectation that higher MGMT activity is associated with TMZ resistance.

MMR acts upon mismatches arising from base misincorporation during DNA replication (5), and also recognizes and processes O^6-MeG:T mispairs

generated by replication past unrepaired O^6-MeG lesions. MMR excises the newly synthesized DNA strand containing T opposite O^6-MeG, but because the methylated lesion remains in place, repair synthesis can restore the O^6-MeG:T mispair, leading to repeated processing by the MMR machinery. This repetitive processing, referred to as futile cycling, mediates the toxicity of S_N1-type alkylating agents by ultimately leading to double strand breaks that activate cell death pathways (6-8). Loss of MMR is therefore associated with MNNG and TMZ resistance in cells (9), and TMZ resistance of tumors *in vivo* (10,11). Furthermore, a recent report indicates that even a modest decrease in MMR capacity can lead to TMZ resistance in GBM (12). Consistent with these data, the negative slope for MMR capacity in models #2, #3, #5, and #6 indicates that *lower* MMR capacity is associated with resistance to TMZ and MNNG. Notably, all of the lymphoblastoid cell lines are MMR proficient relative to a null mutant for MMR (MT1) (13). The data suggest that there may be a continuous relationship between MMR capacity and TMZ sensitivity.

One-sided DNA double strand breaks are generated during a second round of replication past the strand breaks created by MMR-dependent processing of O^6MeG; such double strand breaks can be repaired by the HR pathway (but not the NHEJ pathway), and HR-deficient cells (but not NHEJ deficient cells) exhibit increased sensitivity to S_N1-type alkylating agents (14-16). Furthermore, an acquired chemoresistance mechanism based on the up-regulation of HR has recently been reported (17), and patients with HR deficient lung, breast, and ovarian cancer, which are in some cases treated with alkylating

agents, enjoy prolonged overall survival versus patients with HR proficient cancers (18). Consistent with these observations, the models indicate that cells with higher HR activity are relatively resistant to MNNG and TMZ.

Finally, there is evidence that the NER pathway can process O^6-MeG lesions, as well as 3-methyladenine and 7-methylguanine, which are also generated by S_N1-type alkylating agents (19-21). The positive slopes associated with the NER pathway in the models indicate that higher NER activity is associated with resistance to MNNG and TMZ.

It is notable that the present data in lymphoblastoid cell lines and GBM indicate that the DNA repair-based S_N1-type alkylating agent resistance mechanisms detailed in **Fig. 2** apply not only to cells with profound differences in DRC, such as those achieved when comparing wild type cells versus null mutants, but also to repair-proficient cells that exhibit a continuum of small variations in DRC. This observation suggests that a combination of small changes in DRC in multiple pathways can contribute to the overall sensitivity or resistance of cells to killing with DNA damaging agents.

Repair pathways that contribute to BCNU and MMS sensitivity

One would predict that sensitivity to agents that induce different types of DNA damage will depend upon repair capacity in different DNA repair pathways. Indeed, the MMS and BCNU sensitivity models (#7-10) are distinct from the TMZ and MNNG sensitivity models in several important ways. The lack of a major role for MMR in the BCNU model is consistent with the observation that MMR

deficient cells remain sensitive to BCNU (22). Although major MMR defects caused by mutations in MMR genes lead to resistance to killing with MMS in cancer cell lines (23), less severe MMR defects induced by partial silencing of MSH2 in mouse embryonic fibroblasts had no effect on MMS sensitivity (24). The lack of a major role for MMR in the MMS model is consistent with the observation that small differences in MMR are not associated with major differences in MMS sensitivity (24). In the BCNU MLR model, the MGMT coefficient is by far the largest, the BCNU MLR_L model (#8) excludes all pathways except for MGMT. These models indicate that increased MGMT activity is associated with decreased sensitivity to BCNU. This is consistent with the ability of MGMT to reverse the O^6-chloroethyl DNA adducts formed by BCNU (preventing them from going on to form DNA interstrand crosslinks), and with observations that MGMT-deficient cells are sensitive to BCNU (1). By contrast, MMS is the only agent presently studied for which MGMT does not take the largest coefficient, consistent with the relatively small fraction of O^6-MeG adducts formed by this agent (8). The predominant cytotoxic DNA lesion induced by MMS, 3-methyladenine and, is primarily repaired by the BER pathway, and to a lesser extent by the NER pathway (21). It is important, however, to note that toxic intermediates of this excision repair process can lead to strand breaks that can ultimately be repaired by HR (8). NHEJ defects do not directly lead to MMS hypersensitivity (25), but cells that are deficient for the key NHEJ protein Ku80 are sensitive to MMS (26), and deficient for BER (27). As a result, variation in NHEJ activity that is due to variation in Ku80 levels may correlate with MMS

sensitivity. Consistent with these expectations, the MLR model for MMS sensitivity is dominated by activity in the NER, NHEJ, and HR pathways (BER was not measured in this study). However, following LASSO refinement, only the HR pathway is retained in the MMS MLR_L model (#10), indicating that this pathway is the most important, among those measured, for predicting MMS sensitivity in the lymphoblastoid cell lines. This perhaps underscores the fact that MMS has in some contexts been considered an X-ray mimetic agent (28). Both the BCNU and MMS models feature relatively weak fitting parameters (R^2) relative to the TMZ and MNNG models, suggesting that the inclusion of repair pathways beyond those considered in the present study, might be necessary to make more robust sensitivity predictions for BCNU and MMS.

Limitations of DRC-Based Sensitivity Modeling

Additional data and modeling are needed to determine, for each DNA damaging agent, the combination of repair activities that provides an optimal prediction of sensitivity to cell killing. There is evidence that BER activity plays a role in TMZ sensitivity in GBM (29), suggesting that FM-HCR assays with additional DNA repair substrates might further improve the predictive accuracy of the S_N1-type alkylating agent sensitivity models. When generating models from a training set of cell lines, it is essential that there is variation in both drug sensitivity and repair capacity in the relevant pathways. Although variation among the panel of 24 lymphoblastoid cell lines was sufficient to model DRC-associated changes in drug sensitivity, if applied to a data set with DRC far

outside the range observed in the lymphoblastoid cell lines, the linear models can extrapolate uninterpretable negative numbers or numbers greater than 100% for % control growth. Therefore, an ideal training set for future work might include cell lines specifically engineered to represent the maximum achievable range of DRC for each pathway in living cells.

Supplementary Tables

Table S1. Relative sensitivity of lymphoblastoid cell lines to alkylating agents; values represent percent growth following treatment with DNA damaging agents relative to the untreated controls. Sensitivity to 0.4 mM MMS and 0.5 µg/mL MNNG were measured at 72 hours by manual counting of viable cells after 72 hours (30), and sensitivity to 240 µM TMZ and 40 µM BCNU were determined using a BrdU incorporation assay (31).

Cell Line	MMS	BCNU	MNNG	TMZ
1	9.1	34.5	58.0	72.8
2	25.2	24.2	67.5	ND[1]
3	52.2	35.4	71.6	99.8
4	9.7	1.3	23.1	12.7
5	33.6	4.4	36.5	20.7
6	15.4	32.6	17.8	59.0
7	75.4	14.0	88.0	97.9
8	33.4	43.0	82.8	80.1
9	57.4	20.1	35.5	46.1
10	47.8	40.5	79.7	ND
11	28.9	23.4	41.8	49.6
12	30.8	37.9	82.4	83.7
13	34.9	61.3	71.3	79.7
14	46.5	34.4	75.1	93.5
15	49.4	40.7	43.4	ND
16	61.7	54.4	77.4	87.3
17	47.5	37.1	40.4	78.3
18	33.9	14.4	47.3	ND
19	67.7	39.6	57.0	69.0
20	30.7	18.4	36.3	60.1
21	86.5	51.5	72.9	82.9
22	64.0	44.6	85.0	89.8
23	67.7	40.8	66.1	86.2
24	51.9	44.1	60.3	ND

[1]ND = not determined

Table S2. DNA repair capacity data for 24 cell lines. The values in the table represent percent reporter expression calculated from FM-HCR analysis (13).

Cell Line	NER	MMR	NHEJ	HR	MGMT[1]
1	9.3	3.5	28.2	2.1	0.7
2	9.0	3.2	22.5	2.1	0.4
3	12.2	2.2	29.2	2.3	0.7
4	7.3	2.0	39.7	1.4	29.1
5	7.9	2.4	20.2	1.2	26.2
6	12.4	4.7	27.1	1.9	4.6
7	17.7	3.3	32.1	3.9	1.6
8	10.9	2.1	32.2	2.6	0.2
9	12.8	4.5	22.7	2.5	20.1
10	16.0	1.9	28.7	1.8	5.3
11	9.9	3.2	35.4	1.9	5.4
12	10.0	1.6	22.9	2.8	1.8
13	11.3	3.2	27.7	1.4	0.2
14	19.0	4.3	20.1	2.4	0.1
15	9.0	2.3	28.3	1.8	0.3
16	7.1	2.1	35.0	2.3	0.1
17	22.2	2.7	31.2	2.5	8.1
18	13.9	2.9	28.5	2.8	16.1
19	10.4	2.9	32.9	4.5	8.0
20	12.2	2.8	28.4	2.5	1.6
21	11.6	2.3	40.6	2.2	0.5
22	9.2	2.0	41.6	1.7	0.1
23	14.6	4.8	28.4	2.8	1.0
24	12.2	3.0	34.8	1.4	0.1

[1] Note that for the MGMT assay, higher reporter expression corresponds to lower MGMT activity.

Table S3. Correlation coefficients (R) for pairwise linear relationships between DNA repair capacity in multiple pathways in 24 lymphoblastoid cell lines. For a perfect correlation, R=1; when there is no correlation between the two variables, R=0.

	NER	MMR	NHEJ	HR	MGMT
NER	1.00	0.34	0.20	0.32	0.15
MMR	0.34	1.00	0.40	0.14	0.03
NHEJ	0.20	0.40	1.00	0.02	0.09
HR	0.32	0.14	0.02	1.00	0.17
MGMT	0.15	0.03	0.09	0.17	1.00

Table S4. Statistical significance of linear relationships between DNA repair capacity in multiple pathways in 24 lymphoblastoid cell lines. Calculated p-values for the linear trend between each pair of variables is reported; p-values equal to or less than 0.005 are considered to represent statistically significant linear trends.

	NER	MMR	NHEJ	HR	MGMT
NER		0.10	0.35	0.13	0.48
MMR	0.10		0.05	0.50	0.89
NHEJ	0.35	0.05		0.92	0.67
HR	0.13	0.50	0.92		0.43
MGMT	0.48	0.89	0.67	0.43	

Table S5. Correlation coefficients for pairwise linear relationships between DNA repair capacity and sensitivity to killing with DNA damaging agents in 24 lymphoblastoid cell lines. For a perfect correlation, R=1; when there is no correlation between the two variables, R=0.

	MNNG	**TMZ**	**BCNU**	**MMS**
NER	0.11	0.43	0.03	0.29
Log_{10}(NER)	0.13	0.47	0.06	0.30
MMR	0.31	0.01	0.10	0.03
Log_{10}(MMR)	0.33	0.02	0.12	0.03
NHEJ	0.11	0.06	0.23	0.31
Log_{10}(NHEJ)	0.11	0.09	0.25	0.30
HR	0.27	0.44	0.02	0.43
Log_{10}(HR)	0.29	0.53	0.02	0.41
MGMT	0.62	0.89	0.73	0.28
Log_{10}(MGMT)	0.64	0.78	0.70	0.26

Table S6. Statistical significance of linear relationships between DNA repair capacity and sensitivity to killing with DNA damaging agents in 24 lymphoblastoid cell lines. Calculated p-values for the linear trend between each pair of variables is reported; p-values equal to or less than 0.001 are considered to represent statistically significant linear trends, and are reported in boldface print.

	MNNG	**TMZ**	**BCNU**	**MMS**
NER	0.60	0.07	0.90	0.17
Log_{10}(NER)	0.54	0.04	0.79	0.15
MMR	0.14	0.98	0.63	0.88
Log_{10}(MMR)	0.12	0.94	0.57	0.88
NHEJ	0.60	0.81	0.28	0.14
Log_{10}(NHEJ)	0.62	0.70	0.23	0.16
HR	0.20	0.06	0.91	0.03
Log_{10}(HR)	0.17	0.02	0.94	0.05
MGMT	**0.001**	**< 0.0001**	**< 0.0001**	0.18
Log_{10}(MGMT)	**0.001**	**< 0.0001**	**0.0001**	0.22

Table S7. DNA Repair capacity for indicated repair pathways in PDX models of GBM.

PDX Model	NER	MMR	NHEJ	HR	MGMT[1]
GBM12_5199	5.2	17.8	18.5	8.7	91.0
GBM12TMZ_3080	9.6	19.8	23.6	6.2	0.9
GBM12TMZ_5476	10.4	17.8	14.4	9.4	77.2
GBM14	31.2	8.5	10.2	1.0	9.6
GBM14TMZ	17.7	10.3	12.7	6.3	3.4
GBM22	3.2	12.1	20.4	5.4	94.9
GBM22TMZ	4.8	0.5	17.1	13.4	98.0
GBM39	20.0	18.6	2.6	1.5	92.2
GBM39TMZ	32.7	6.5	8.6	2.3	103.3
GBM59	11.9	11.4	7.5	3.4	56.6
GBM59TMZ	19.5	3.9	2.3	5.6	70.8
GBM46	38.9	3.6	5.8	1.4	80.2

[1] Note that for the MGMT assay, higher reporter expression corresponds to lower MGMT activity.

Supplemental Figures

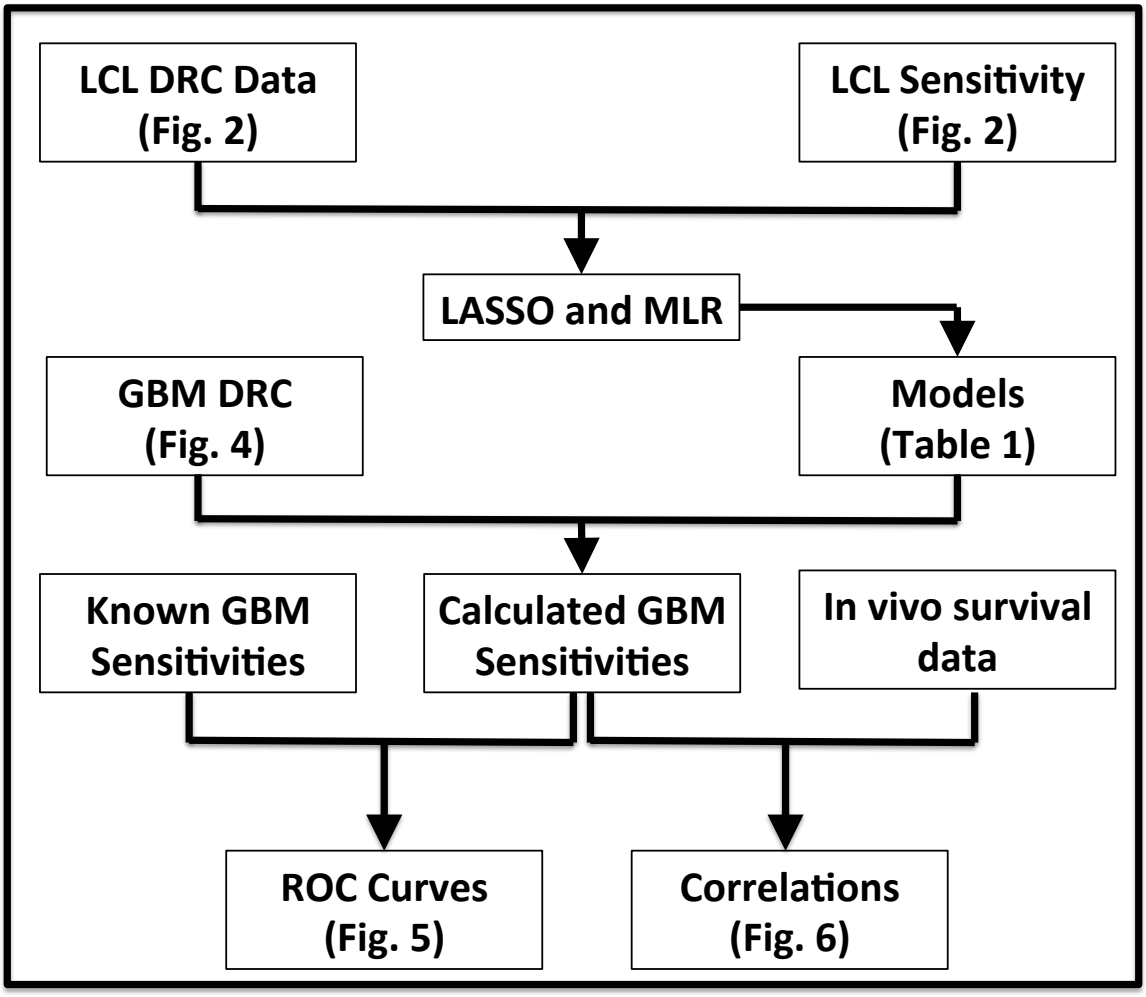

Figure S1. Computational Workflow. Figures and Tables in which the data or computational results can be found are indicated. Lymphoblastoid cell lines are abbreviated "LCL".

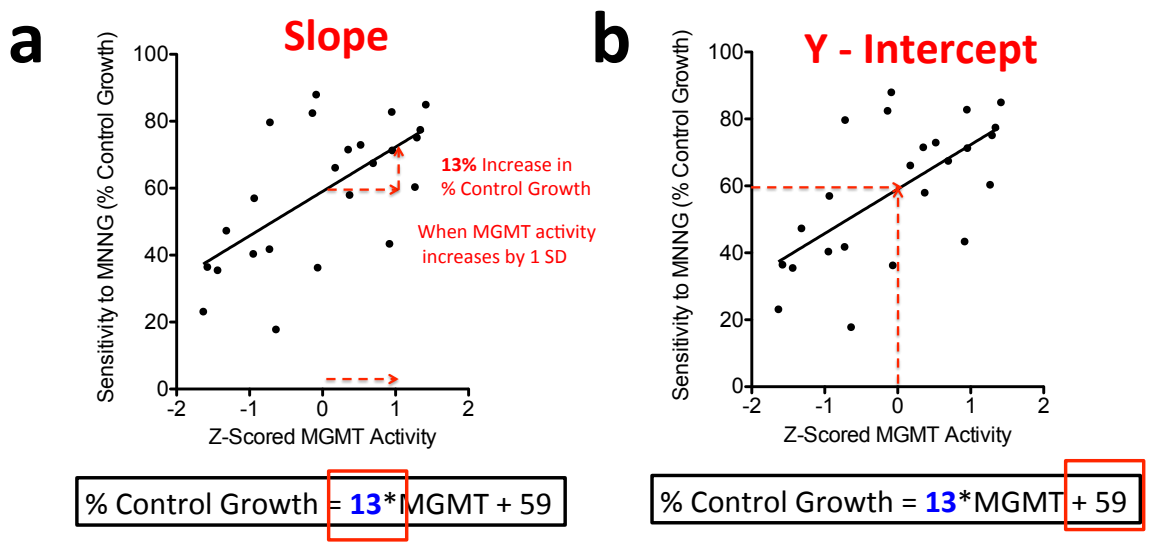

Figure S2. Diagram of a linear model relating MGMT activity to sensitivity to MNNG. a) The slope of the linear model corresponds to the change in sensitivity (measured as % Control Growth) when repair capacity changes by 1 standard deviation. For this model, a 1 standard deviation increase in MGMT activity yields an increase in % Control Growth of 13%. b) The constant at the end of the linear model represents that point at which the linear model crosses the y-axis. Note that in this plot, the y-axis has been displaced from the origin to facilitate visualization of the data. For a two dimensional model, the data are fit to a plane instead of a line; for higher dimensional models the data are fit to hyperplanes that are not amenable to representation in 3-dimensional coordinate space. Nevertheless, the geometric interpretations of slope and intercept illustrated here can be generalized to multiple linear models.

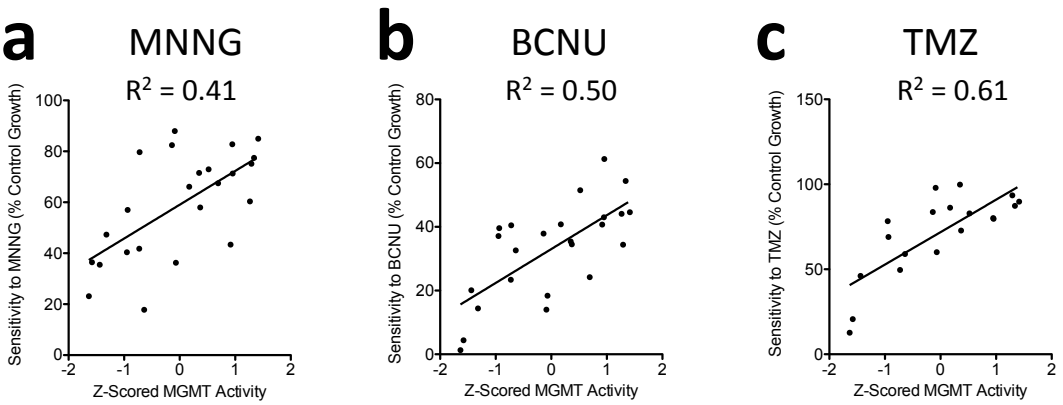

Figure S3. Correlation between MGMT activity (as measured by FM-HCR) and sensitivity to a DNA damaging agent. MGMT activity was calculated from the logarithm of % reporter expression for the MGMT reporter (**Table S2**), followed by Z-scoring. Because % reporter expression is inversely related to MGMT activity, Z-scored MGMT values were multiplied by -1. Sensitivity is reported as % growth following treatment with DNA damaging agents relative to the controls (Table S1).

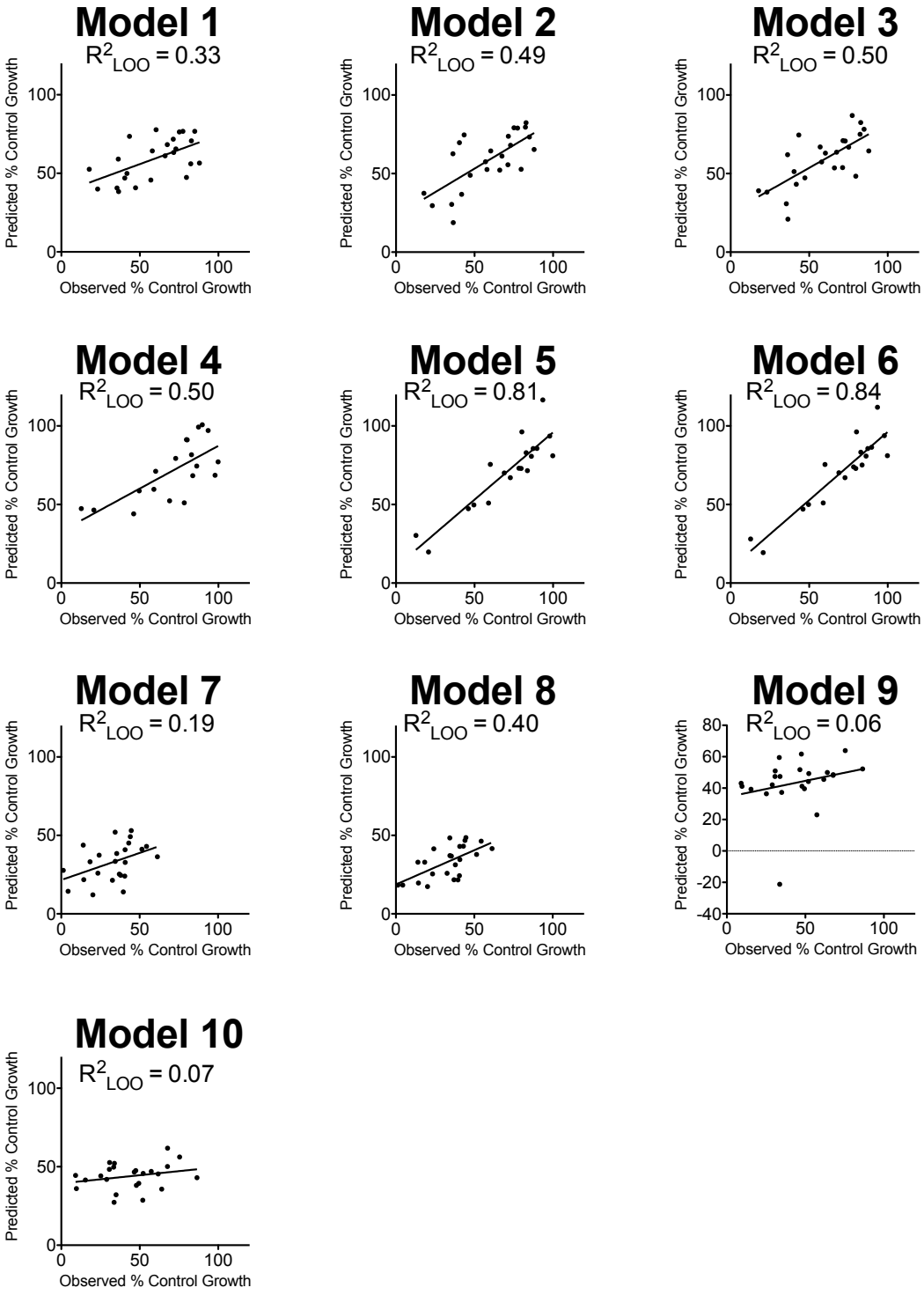

Figure S4. Scatter plots of observed sensitivity (% Control Growth) versus predicted sensitivity calculated from leave-one-out analysis of the models listed in **Table 1**.

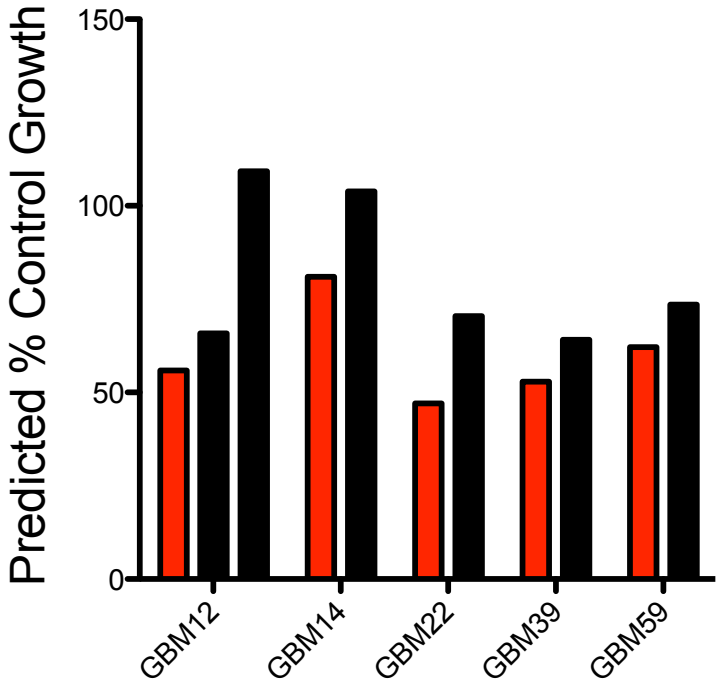

Figure S5. Predicted and observed sensitivity of paired GBM xenograft lines with differential TMZ sensitivities. Predicted relative TMZ sensitivities of parental (Sensitive; red) and acquired resistance models (Resistant, black). For each pair, a relative increase in predicted % control growth was correctly predicted for the PDX models that acquired TMZ resistance. Sensitivity to killing with TMZ was calculated using Z-scored DNA repair capacity data from **Table S7**.

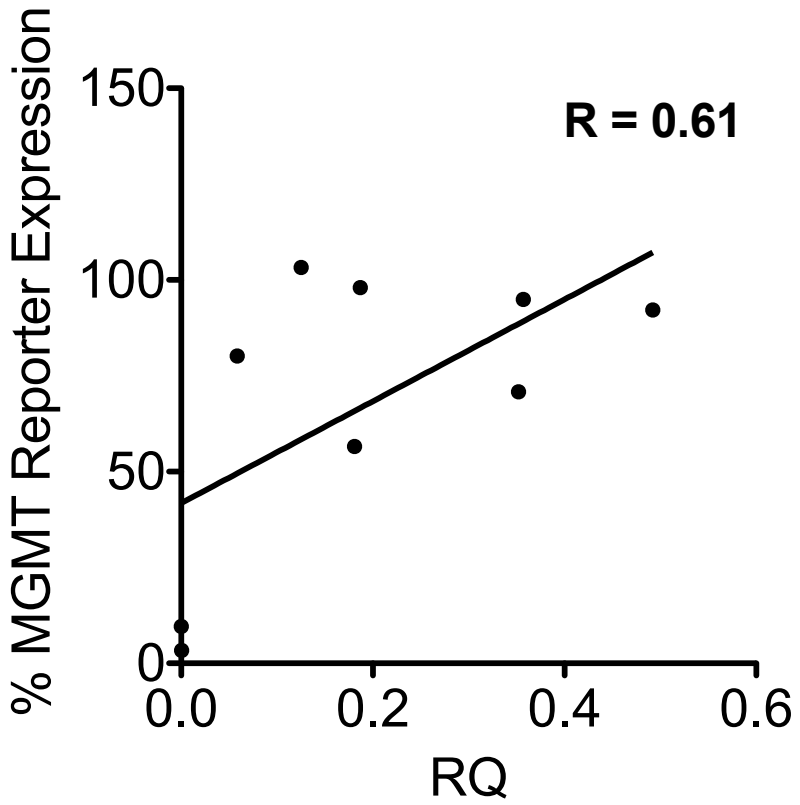

Figure S6. Correlation between MGMT activity and promoter methylation status. RQ represents the relative quantity of methylation assayed by methylation specific PCR; data are normalized to a positive control for methylation generated by treating genomic DNA with CpG methyltransferase M.SssI. Note that higher levels of % MGMT reporter expression correspond to lower levels of MGMT activity.

Scripts

Multiple Linear Regression

```
[b,bint,r,rint,stats] = regress(y,X) %Performs MLR
for(i=1:24)
    ev = X(i, :); % Defines the excluded variable as row i in matrix X,
and semicolon is used to suppress the result appearing in the command
window
    iv = []; % defines the included variable
    for j = 1:24
        if j ~= i
            iv = [iv j];
        end % this ends the first step for i = 1; make the first vector
where j = 1, iv will now be [2]
    end % this ends the loop that builds the vector iv when we reach i
= 24, and iv = [2 3 4 …]
 [newX] = X(iv, :);
 % This creates a new X matrix indexed to the vector iv; if for example
row
 % 10 is missing from y, row 10 will be excluded from newX
 [newy] = y(iv, :);
 [b,bint,r,rint,stats] = regress(newy,newX);
 pred = dot(b,ev);
 % we regress the new vector and i = 1 left out
 % calculates the response (pred) for ev, the excluded variable using
the new slopes, b.  We take
 % the dot product of the two vectors
 predvector(i) = pred(:); %This is the vector of the predicted values
from the leave one out analysis
 % the loop continues with i = 2 and so forth, until we have repeated
the process through i = 24
end
```

LASSO Selection of Variables and Subsequent MLR

```
Performs Lasso with leave-one-out cross-validation for
% the predictor variables retained at each value of lambda
predvector=[] % clears a vector of previous values
MLR % performs multiple linear regression DRC data X, sensitivity data
y
LASSO; % performs LASSO
B(end:end,:)=[1]; % replace the last row of the LASSO output matrix
with a row of 1's
M = size(B,2);
sz = size(y,1);
for k=1:(M-1) % This loop creates a logical index for coefficients
associated
    % with each LASSO lambda value
    F = B(:,k); % Define vectors from each column of the LASSO output
of slopes, b
    G = logical(F); % Convert vector F to logical index G
    lX = X(:,G); % Index the predictor variable set to G
    for(i=1:sz)
```

```
    ev = lX(i, :); % Defines the excluded variable as row i in matrix
X,
    ey = y(i, :);
    iv = []; % defines the included variable
    for j = 1:sz
        if j ~= i
            iv = [iv j];
        end % this ends the first step for i = 1; make the first vector
where j = 1, iv will now be [2]
    end % this ends the loop that builds the vector iv when we reach i
= 24, and iv = [2 3 4 ...]
 [newX] = lX(iv, :);
 % This creates a new X matrix indexed to the vector iv; if for example
row
 % 10 is missing from y, row 10 will be excluded from newX
 [newy] = y(iv, :);
 [b,bint,r,rint,stats] = regress(newy,newX);
 pred = dot(b,ev);
 mvector(i) = mse(pred, ey); %This creates a vector of MSE values
indexed to the step in the loop
 % we regress the new vector and i = 1 left out
 % calculates the response (pred) for ev, the excluded variable using
the new slopes, b.  We take
 % the dot product of the two vectors
 predvector(i) = pred(:); %This is the vector of the predicted values
from the leave one out analysis
 % the loop continues with i = 2 and so forth, until we have repeated
the process through i = 24
end
mdl = fitlm(y, predvector); %Fits a linear model to the measured values
y versus the predicted values predvector
Rnow(k) = sqrt(mdl.Rsquared.Ordinary); %Reports R for the correlation
between y and predvector
MSEnow(k) = sum(mvector)/sz; %Calculates the average of the MSE from
each step, which represents the MSE for the entire cross-validation
mat(k,:) = predvector;
MAT = transpose(mat); % Reports the predicted sensitivities from cross-
validation
end
Z = min(MSEnow); % Defines the step at which MSE is lowest
 Min_MSE = find(MSEnow==Z);
 ind=min(Min_MSE)
 F=B(:,ind);
 G = logical(F);
lX = X(:,G);
[b,bint,r,rint,stats] = regress(y,lX); % Performs MLR using the
variables selected by LASSO
```

Supplemental References

1. Pegg AE. Multifaceted Roles of Alkyltransferase and Related Proteins in DNA Repair, DNA Damage, Resistance to Chemotherapy, and Research Tools. *Chem Res Toxicol* **2011**;24:618-39.
2. Watts GS, Pieper RO, Costello JF, Peng YM, Dalton WS, Futscher BW. Methylation of discrete regions of the O-6-methylguanine DNA methyltransferase (MGMT) CpG island is associated with heterochromatinization of the MGMT transcription start site and silencing of the gene. *Mol Cell Biol* **1997**;17:5612-19.
3. van Nifterik KA, van den Berg J, van der Meide WF, Ameziane N, Wedekind LE, Steenbergen RDM, et al. Absence of the MGMT protein as well as methylation of the MGMT promoter predict the sensitivity for temozolomide. *Br J Cancer* **2010**;103:29-35.
4. Hegi ME, Diserens A, Gorlia T, Hamou M, de Tribolet N, Weller M, et al. MGMT gene silencing and benefit from temozolomide in glioblastoma. *New England Journal of Medicine* **2005**;352:997-1003.
5. Li G-M. Mechanisms and functions of DNA mismatch repair. *Cell Research* **2008**;18:85-98.
6. Quiros S, Roos WP, Kaina B. Processing of O-6-methylguanine into DNA double-strand breaks requires two rounds of replication whereas apoptosis is also induced in subsequent cell cycles. *Cell Cycle* **2010**;9:168-78.
7. Mojas N, Lopes M, Jiricny J. Mismatch repair-dependent processing of methylation damage gives rise to persistent single-stranded gaps in newly replicated DNA. *Genes Dev* **2007**;21:3342-55.
8. Fu D, Calvo JA, Samson LD. Balancing repair and tolerance of DNA damage caused by alkylating agents. *Nat Rev Cancer* **2012**;12:104-20.
9. Kat A, Thilly WG, Fang WH, Longley MJ, Li GM, Modrich P. An alkylation-tolerant, mutator human cell line is deficient in strand-specific mismatch repair *Proceedings of the National Academy of Sciences of the United States of America* **1993**;90:6424-28.
10. Cahill DP, Levine KK, Betensky RA, Codd PJ, Romany CA, Reavie LB, et al. Loss of the mismatch repair protein MSH6 in human glioblastomas is associated with tumor progression during temozolomide treatment. *Clinical Cancer Research* **2007**;13:2038-45.
11. Felsberg J, Thon N, Eigenbrod S, Hentschel B, Sabel MC, Westphal M, et al. Promoter methylation and expression of MGMT and the DNA mismatch repair genes MLH1, MSH2, MSH6 and PMS2 in paired primary and recurrent glioblastomas. *International Journal of Cancer* **2011**;129:659-70.
12. McFaline-Figueroa JL, Braun CJ, Stanciu M, Nagel ZD, Mazzucato P, Sangaraju D, et al. Minor changes in expression of the mismatch repair protein MSH2 exert a major impact on glioblastoma response to temozolomide. *Cancer Res* **2015**.
13. Nagel ZD, Margulies CM, Chaim IA, McRee SK, Mazzucato P, Ahmad A, et al. Multiplexed DNA repair assays for multiple lesions and multiple doses via transcription inhibition and transcriptional mutagenesis. *Proceedings of the*

National Academy of Sciences of the United States of America **2014**;111:E1823-32.
14. Short SC, Giampieri S, Worku M, Alcaide-German M, Sioftanos G, Bourne S, et al. Rad51 inhibition is an effective means of targeting DNA repair in glioma models and CD133+tumor-derived cells. *Neuro-Oncology* **2011**;13:487-99.
15. Quiros S, Roos WP, Kaina B. Rad51 and BRCA2-New Molecular Targets for Sensitizing Glioma Cells to Alkylating Anticancer Drugs. *Plos One* **2011**;6.
16. Roos WP, Nikolova T, Quiros S, Naumann SC, Kiedron O, Zdzienicka MZ, et al. Brca2/Xrcc2 dependent HR, but not NHEJ, is required for protection against O(6)-methylguanine triggered apoptosis, DSBs and chromosomal aberrations by a process leading to SCEs. *DNA Repair (Amst)* **2009**;8:72-86.
17. Ohba S, Mukherjee J, See WL, Pieper RO. Mutant IDH1-Driven Cellular Transformation Increases RAD51-Mediated Homologous Recombination and Temozolomide Resistance. *Cancer Research* **2014**;74:4836-44.
18. Peng G, Lin CC-J, Mo W, Dai H, Park Y-Y, Kim SM, et al. Genome-wide transcriptome profiling of homologous recombination DNA repair. *Nature Communications* **2014**;5.
19. Samson L, Thomale J, Rajewsky MF. Alternative pathways for the in vivo repair of O6-alkylguanine and O4-alkylthymine in Escherichia coli: the adaptive response and nucleotide excision repair. *Embo j* **1988**;7:2261-7.
20. Huang JC, Hsu DS, Kazantsev A, Sancar A. Substrate spectrum of human excinuclease: repair of abasic sites, methylated bases, mismatches, and bulky adducts. *Proc Natl Acad Sci U S A* **1994**;91:12213-7.
21. Plosky B, Samson L, Engelward BP, Gold B, Schlaen B, Millas T, et al. Base excision repair and nucleotide excision repair contribute to the removal of N-methylpurines from active genes. *DNA Repair (Amst)* **2002**;1:683-96.
22. Hickman MJ, Samson LD. Role of DNA mismatch repair and p53 in signaling induction of apoptosis by alkylating agents. *Proceedings of the National Academy of Sciences of the United States of America* **1999**;96:10764-69.
23. Glaab WE, Risinger JI, Umar A, Barrett JC, Kunkel TA, Tindall KR. Cellular resistance and hypermutability in mismatch repair-deficient human cancer cell lines following treatment with methyl methanesulfonate. *Mutat Res-Fundam Mol Mech Mutagen* **1998**;398:197-207.
24. Cooley N, Elder RH, Povey AC. The effect of Msh2 knockdown on methylating agent induced toxicity in DNA glycosylase deficient cells. *Toxicology* **2010**;268:111-17.
25. Lundin C, North M, Erixon K, Walters K, Jenssen D, Goldman AS, et al. Methyl methanesulfonate (MMS) produces heat-labile DNA damage but no detectable in vivo DNA double-strand breaks. *Nucleic Acids Res* **2005**;33:3799-811.
26. Nussenzweig A, Sokol K, Burgman P, Li L, Li GC. Hypersensitivity of Ku80-deficient cell lines and mice to DNA damage: the effects of ionizing radiation on growth, survival, and development. *Proc Natl Acad Sci U S A* **1997**;94:13588-93.
27. Li H, Marple T, Hasty P. Ku80-deleted cells are defective at base excision repair. *Mutat Res* **2013**;745-746:16-25.

28. Serres FJ, Shelby MD. Comparative Chemical Mutagenesis. [electronic resource]. Boston, MA : Springer US, 1982.; 1982.
29. Trivedi RN, Wang XH, Jelezcova E, Goellner EM, Tang JB, Sobol RW. Human methyl purine DNA glycosylase and DNA polymerase beta expression collectively predict sensitivity to temozolomide. *Molecular pharmacology* **2008**;74:505-16.
30. Fry RC, Svensson JP, Valiathan C, Wang E, Hogan BJ, Bhattacharya S, et al. Genomic predictors of interindividual differences in response to DNA damaging agents. *Genes Dev* **2008**;22:2621-26.
31. Valiathan C, McFaline JL, Samson LD. A rapid survival assay to measure drug-induced cytotoxicity and cell cycle effects. *DNA Repair* **2012**;11:92-98.